

Clinical Significance of Tumor-Associated Inflammatory Cells in Metastatic Neuroblastoma

Shahab Asgharzadeh, Jill A. Salo, Lingyun Ji, André Oberthuer, Matthias Fischer, Frank Berthold, Michael Hadjidanis, Cathy Wei-Yao Liu, Leonid S. Metelitsa, Roger Pique-Regi, Peter Wakamatsu, Judith G. Villablanca, Susan G. Kreissman, Katherine K. Matthay, Hiroyuki Shimada, Wendy B. London, Richard Spoto, and Robert C. Seeger

A B S T R A C T

Purpose

Children diagnosed at age ≥ 18 months with metastatic *MYCN*-nonamplified neuroblastoma (NBL-NA) are at high risk for disease relapse, whereas those diagnosed at age < 18 months are nearly always cured. In this study, we investigated the hypothesis that expression of genes related to tumor-associated inflammatory cells correlates with the observed differences in survival by age at diagnosis and contributes to a prognostic signature.

Methods

Tumor-associated macrophages (TAMs) in localized and metastatic neuroblastomas ($n = 71$) were assessed by immunohistochemistry. Expression of 44 genes representing tumor and inflammatory cells was quantified in 133 metastatic NBL-NAs to assess age-dependent expression and to develop a logistic regression model to provide low- and high-risk scores for predicting progression-free survival (PFS). Tumors from high-risk patients enrolled onto two additional studies ($n = 91$) served as independent validation cohorts.

Results

Metastatic neuroblastomas had higher infiltration of TAMs than locoregional tumors, and metastatic tumors diagnosed in patients at age ≥ 18 months had higher expression of inflammation-related genes than those in patients diagnosed at age < 18 months. Expression of genes representing TAMs (*CD33/CD16/IL6R/IL10/FCGR3*) contributed to 25% of the accuracy of a novel 14-gene tumor classification score. PFS at 5 years for children diagnosed at age ≥ 18 months with NBL-NA with a low- versus high-risk score was 47% versus 12%, 57% versus 8%, and 50% versus 20% in three independent clinical trials, respectively.

Conclusion

These data suggest that interactions between tumor and inflammatory cells may contribute to the clinical metastatic neuroblastoma phenotype, improve prognostication, and reveal novel therapeutic targets.

J Clin Oncol 30:3525-3532. © 2012 by American Society of Clinical Oncology

INTRODUCTION

The concept of tumor-promoting inflammation is a recognized enabling characteristic of cancers.¹ Recent studies have demonstrated the prognostic significance of tumor-associated macrophages (TAMs) in some adult cancers, including Hodgkin's lymphoma and breast cancer.²⁻⁶ However, the prognostic significance of tumor-associated inflammatory cells in metastatic disease and in childhood cancers is unknown.

Neuroblastoma, an embryonal tumor of the sympathetic nervous system, is one of the most common solid tumors in children, with approximately 40% of patients presenting with metastatic disease at

diagnosis.⁷ Among those with metastatic disease, amplification of the *MYCN* proto-oncogene (30% of tumors) is associated with high risk of disease relapse, whereas those lacking *MYCN* amplification (NBL-NA) have clinical behaviors that are distinctly associated with age at diagnosis.⁸⁻¹⁰ Patients diagnosed with metastatic NBL-NA at age ≥ 18 months often have tumors with recurrent segmental genomic alterations and have high-risk disease with only 45% long-term disease-free survival.¹⁰⁻¹⁶ In contrast, children diagnosed with metastatic NBL-NA at age < 18 months of age frequently have tumors with whole chromosomal alterations and have greater than 90% overall survival (OS) after receiving only moderate-intensity chemotherapy.¹⁷⁻²⁰

Shahab Asgharzadeh, Jill A. Salo, Michael Hadjidanis, Cathy Wei-Yao Liu, Peter Wakamatsu, Judith G. Villablanca, Hiroyuki Shimada, Richard Spoto, and Robert C. Seeger, Children's Hospital Los Angeles and Saban Research Institute; Shahab Asgharzadeh, Lingyun Ji, Judith G. Villablanca, Hiroyuki Shimada, Richard Spoto, and Robert C. Seeger, Keck School of Medicine, University of Southern California, Los Angeles; Katherine K. Matthay, University of California School of Medicine and University of California, San Francisco, Benioff Children's Hospital, San Francisco; Wendy B. London, Children's Oncology Group, Arcadia, CA; Wendy B. London, Children's Hospital Boston/Dana-Farber Cancer Institute, Boston, MA; André Oberthuer, Matthias Fischer, and Frank Berthold, Children's Hospital, University of Cologne, and Center for Molecular Medicine Cologne, Cologne, Germany; Leonid S. Metelitsa, Baylor College of Medicine, Houston, TX; Roger Pique-Regi, University of Chicago, Chicago, IL; and Susan G. Kreissman, Duke University Medical Center, Durham, NC.

Submitted November 29, 2011; accepted June 29, 2012; published online ahead of print at www.jco.org on August 27, 2012.

Supported by Grant No. 2R01 CA60104-16 from the National Cancer Institute (R.C.S.), a grant from Amgen (J.A.S.), Grant No. K12-CA60104 from the National Institute of Child Health and Human Development, grants from Alex's Lemonade Stand Foundation and St Baldrick's Foundation (S.A.), and grants from the Nautica Malibu Triathlon and Bogart Pediatric Cancer Research Program (S.A., R.C.S.).

Authors' disclosures of potential conflicts of interest and author contributions are found at the end of this article.

Corresponding author: Shahab Asgharzadeh, MD, 4650 Sunset Blvd, MS 57, Los Angeles, CA 90027; e-mail: sasgharzadeh@chla.usc.edu.

© 2012 by American Society of Clinical Oncology

0732-183X/12/3028-3525/\$20.00

DOI: 10.1200/JCO.2011.40.9169

Biologic mechanisms responsible for the age-dependent genomic and clinical phenotypes of metastatic NBL-NA and for different responses to treatment among those age ≥ 18 months at diagnosis have been unclear.

Our previous gene expression profiling study of metastatic NBL-NA tumors suggested that there may be age-dependent differences in expression of genes representing tumor-associated inflammatory cells.²¹ In the current study, we focused on intratumor inflammatory cells, especially TAMs, and their relationship with clinical behavior of metastatic NBL-NA. We examined the infiltration of macrophages in locoregional and metastatic tumors with immunohistochemistry (IHC). We also used a TaqMan low-density array (TLDA; Life Technologies, Carlsbad, CA) assay to assess expression of inflammatory and tumor cell-related genes in metastatic NBL-NA tumors diagnosed before and after 18 months of age. Our findings provide new insights about intratumor inflammation in metastatic NBL-NA tumors and provide the basis for constructing a novel 14-gene model that predicts risk of disease progression in those diagnosed at age ≥ 18 months.

METHODS

Tissue microarray (TMA) details are provided in the Data Supplement. Macrophages were identified using IHC analysis of primary neuroblastoma tissues using antibodies directed against CD163 and allograft inflammatory factor 1 (AIF1). Tissue section scores ranged from 0 to 7 for each marker, with higher scores indicating a greater proportion of positive cells.

The details of the 48-gene TLDA assay are provided in the Data Supplement. All patients included in the gene expression study had metastatic NBL-NA tumors and were enrolled onto Children's Cancer Group (CCG), German Society for Pediatric Oncology-Hematology (GPOH), or Children's Oncology Group (COG) trials at diagnosis (Table 1 and Data Supplement). Details of treatment for the three cohorts were described previously and are provided in the Data Supplement.^{12,14,16,21} Informed consent was obtained in accordance with institutional review board policies.

Statistical Analysis

The Data Supplement illustrates the flow of statistical and validation methods used in this report. Because our primary interest was to identify genes that are predictive of outcome in the cohort of patients older than 18 months of age, we first conducted a univariate logistic regression model based on TLDA gene expression data from 133 samples from the training cohort (CCG), which includes patients older and younger than 18 months of age at the time of diagnosis. Genes that were independent of age at diagnosis with a *P* value of $\leq .25$ were included in a final multivariate logistic model to predict PFS. Our aim was to build a robust model that was predictive of disease progression in patients older than 18 months of age and that could be used as the basis for classification into signature-based low- and high-risk tumor-progression groups. Disease progression was defined a priori (Data Supplement). The effective period for risk of disease progression in the training cohort was 4 years from diagnosis. Because few patients were censored before the end of the effective period for risk of disease progression, ignoring this censoring had little practical effect on the logistic regression analysis of whether disease progression had occurred. Age was included as a continuous covariate in the final multivariate logistic regression analysis to assess for residual significance. Logit values, representing the tumor-progression scores, were computed for each patient. Measures of accuracy based on resubstitution analysis and leave-one-out cross validation (LOOCV) are presented. Classification accuracy was assessed using receiver operating characteristic curves and areas under the curve (AUC). External validation of the prediction model was performed using the independent GPOH and COG samples, with the tumor-progression score for each patient calculated using the regression coefficients from the prediction model derived from the training cohort. The relative contributions to the accuracy of the 14-gene NBL-NA prediction score of age at diagnosis, tumor cell-related genes, and inflammation-related genes were assessed using 5,000 permutations of the data set (Data Supplement).

Tumor-progression risk scores obtained from the multivariate logistic regression model were used to define signature-based risk groups. The median tumor-progression risk score from the training cohort ($n = 133$) was used as the cutoff point to define signature-based high-risk (tumor-progression score \geq median score) or low-risk (tumor-progression score $<$ median score) scores.

Table 1. Characteristics of Patients With Metastatic Neuroblastoma Lacking *MYCN* Gene Amplification

Characteristic	Training Cohort (age at diagnosis, months)				Validation Cohorts (age at diagnosis, months)			
	CCG				GPOH		COG	
	< 18 ($n = 39$)		≥ 18 ($n = 94$)		≥ 18 ($n = 39$)		≥ 18 ($n = 52$)	
	No.	%	No.	%	No.	%	No.	%
Age at diagnosis, months								
Mean	9.3		53.6		56		55.9	
Range	0.1-17.3		18.2-151		18.4-182		19.5-186	
COG risk stratification	Intermediate*		High		High		High	
INPC classification								
Favorable	34	87	2	2	3	8	3	6
Unfavorable	5	13	91	97	34	87	42	81
Unknown	0	0	1	1	2	5	7	13
Clinical trials	323P, 3881		323P, 321-2, 321-3, 3891		NB90, NB95, NB97, NB2004		A3973†	
5-year EFS rate, %	95		23		34		31	
95% CI, %	81 to 99		15 to 32		19 to 50		19 to 44	
5-year OS rate, %	95		35		50		38	
95% CI, %	81 to 99		25 to 44		32 to 66		23 to 54	

Abbreviations: CCG, Children's Cancer Group; COG, Children's Oncology Group; EFS, event-free survival; GPOH, German Society for Pediatric Oncology-Hematology (Gesellschaft für Pädiatrische Onkologie und Hämatologie); INPC, International Neuroblastoma Pathology Classification; OS, overall survival.

*Patients age > 12 months were classified as high risk and treated accordingly per CCG guidelines. On the basis of current COG guidelines, four of 12 patients diagnosed at 12 to 18 months of age with unfavorable tumor histology would be considered high risk.

†Three patients were treated on ANBL0532.

Statistical Methods

Details of the statistical analyses for developing the prognostic score are described here and summarized in the Data Supplement. In addition, survival analysis methods²² are used to describe outcome in low- and high-risk groups defined by the prognostic score. The primary end point for these analyses was progression-free survival (PFS), defined as the minimum interval from date of diagnosis to date of disease progression, date of death (four patients only), or date of last follow-up. Patients who did not experience progression or die were censored at the time of last follow-up. The Kaplan-Meier method was used to compute PFS probabilities and produce survival curves. CIs are based on Greenwood SEs. Unless otherwise stated, the reported probabilities are based on 5-year PFS rates. Tests of the difference in PFS between risk groups are based on the log-rank statistic. Other common statistics²³ (eg, *t* test, Spearman rank correlation) were used where appropriate and are indicated in the text. Bonferroni adjustments to account for multiple comparisons were used where appropriate. Statistical computations were performed using STATA software (version 9.0; STATA, College Station, TX) or the R project (<http://www.r-project.org>).

RESULTS

Infiltration of Inflammatory Cells in Metastatic Neuroblastoma

We performed IHC analysis of 71 neuroblastoma tumors (29 patients with locoregional, 31 with metastatic disease [stage 4], and 11 with metastatic disease with special designation [stage 4S]; Data Supplement) using antibodies directed against two macrophage markers (CD163 and AIF1). There were significantly greater numbers of infiltrating macrophages observed only with *CD163* staining, which identifies alternatively activated macrophage (M2), in samples of patients with metastatic (stage 4) compared with locoregional neuroblastoma (*t* test $P = .003$; Bonferroni-adjusted $P < .017$ considered significant; Fig 1A). There was no statistically significant difference in the number of intratumor CD163+ macrophages between metastatic tumors with

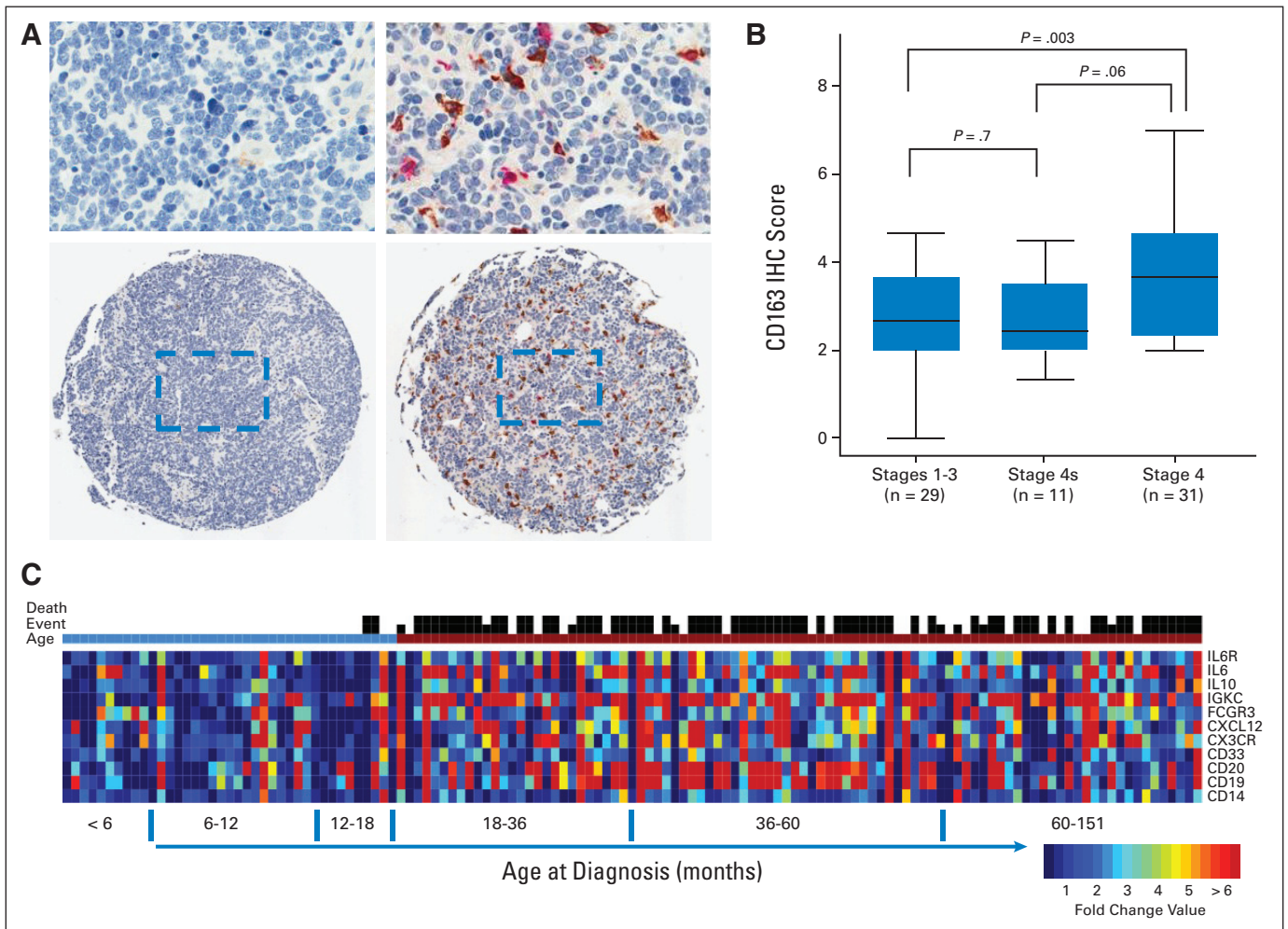


Fig 1. Evidence of tumor-associated macrophages and inflammation in neuroblastoma. (A) Representative immunohistochemical analyses of staining of CD163 (brown staining) and AIF1 (red staining) in primary tumor samples from a patient with stage 1 tumor (left panel) lacking any infiltrating macrophages and a patient with metastatic disease (right panel) with extensive infiltration of CD163+ macrophages. (B) Average scores for the presence of CD163+ infiltrating macrophages reveals significant infiltration in tumor samples of patients with metastatic disease compared with those with locoregional tumors. Patients with stage 4S tumors, who are known to undergo spontaneous regression, had CD163+ macrophages comparable to those with locoregional tumors (Bonferroni adjusted $P < .017$ considered significant). (C) Heatmap of gene expression levels of inflammation-related genes displayed along increasing age at diagnosis of 133 children with metastatic *MYCN*-nonamplified neuroblastoma. Heatmap colors reflect fold-change value of individual tumor relative to the average expression level of inflammation-related genes in children diagnosed at age < 18 months. Occurrences of an event and of death are indicated by black vertical bars above the color-coded bar for age at diagnosis.

Table 2. Characteristics and Prognostic Significance of the 14 Genes of the Neuroblastoma Signature

Symbol	Gene Name	Gene Location	Univariate OR	95% CI†	P	Prediction Accuracy (AUC; CCG patients age \geq 18 months)‡
Tumor-related genes						
<i>H2AFV</i>	H2A histone family, member V	7p13	0.42	0.26 to 0.68	< .001	0.6275
<i>GPATC4</i>	G patch domain containing 4	1q22	2.08	1.33 to 3.24	< .001	0.6060
<i>PTPN5</i>	Protein tyrosine phosphatase, nonreceptor type 5	11p15.1	1.28	1.10 to 1.48	< .001	0.5636
<i>PGM2L1</i>	Phosphoglucomutase 2-like 1	11q13.4	0.62	0.45 to 0.85	.002	0.5127
<i>GFRA3</i>	GDNF family receptor alpha 3	5q31.1	0.79	0.62 to 1.01	.05	0.4729
<i>THAP2</i>	THAP domain containing, apoptosis-associated protein 2	12q21.1	0.59	0.34 to 1.03	.05	0.4703
<i>BTBD3</i>	BTB (POZ) domain containing 3	20p12.2	0.76	0.56 to 1.02	.06	0.4514
<i>CAMTA1</i>	Calmodulin-binding transcription activator 1	1p36.31	0.80	0.60 to 1.05	.1	0.4494
<i>NTRK2</i>	Neurotrophic tyrosine kinase receptor type 2	9q22.1	1.16	0.91 to 1.48	.2	0.4886
Inflammation-related genes						
<i>FCGR3 (CD16)</i>	Fc fragment of immunoglobulin G, CD16	1q23	1.36	1.08 to 1.72	.006	0.5649
<i>IL-6R</i>	Interleukin-6 receptor	1q21	1.26	0.97 to 1.65	.08	0.4977
<i>CD33</i>	CD33 antigen	19q13.3	1.34	1.00 to 1.80	.04	0.5179
<i>IL-10</i>	Interleukin-10	1q31-q32	1.17	0.91 to 1.50	.2	0.4814
<i>CD14</i>	CD14 antigen	5q31.1	1.25	0.92 to 1.70	.15	0.5036

Abbreviations: AUC, area under the curve; CCG, Children's Cancer Group; OR, odds ratio; ROC, receiver operating characteristic curve.

*Univariate OR for each gene after adjusting for age at diagnosis for the training CCG cohort (n = 133). Coefficients were calculated based on a two-fold increase in gene expression (ie, equivalent to a change of 1 Δ CT).

†AUC values are reported for the patients diagnosed at age \geq 18 months in the training cohort. A logistic regression model that included the individual gene expression value plus age at diagnosis as a continuous variable was fit to the training cohort (n = 133). The logit scores were used in ROC analysis to obtain AUC values.

special designation (stage 4S), which undergo spontaneous regression, and locoregional tumors (Fig 1B).

We also performed gene expression analysis of 133 metastatic NBL-NA tumors (CCG cohort: 94 children diagnosed at age \geq 18 months and 39 diagnosed at age < 18 months; Table 1; Data Supplement) with a custom-built TLDA containing 31 tumor-related and 13 inflammation-related genes (Data Supplement). We identified greater expression of inflammation-related genes associated with monocyte/macrophage, myeloid, and B cells in tumors of children diagnosed at age \geq 18 months compared with those diagnosed at age < 18 months (Fig 1C). Although inflammation-related genes *CD33*, *FCGR3 (CD16)*, and *IGKC* showed significant association with PFS in univariate analysis (Data Supplement), we did not identify any single gene model that could accurately predict PFS in children diagnosed at age \geq 18 months with AUC > 0.7. These data suggest that inflammatory cells within tumors, especially TAMs, contribute to the age-associated clinical behavior of metastatic NBL-NA tumors.

Expression of Inflammation- and Tumor Cell-Related Genes Comprises a Prognostic Signature

We further examined the expression of the 31 tumor-related and 13 inflammation-related genes in the CCG cohort and identified 14 genes that contributed to a model predictive of PFS (Table 2). Among the 14 genes used in our model, nine (64%) were tumor cell related, and five (36%) were inflammation related. The accuracy of the model for predicting PFS using LOOCV AUC estimates was 0.82 for patients in all age groups and 0.74 for patients age \geq 18 months at diagnosis (Data Supplement).

Tumors from the CCG cohort were categorized as low or high risk based on their 14-gene tumor-progression risk score using LOOCV analysis. Figures 2A and 2B show that patients with a low-risk score had significantly better PFS (72% at 5 years; 95% CI, 60% to 82%) than those in the high-risk score group (16% at 5 years; 95% CI,

8% to 26%) using LOOCV analysis ($P < .001$). The overall 5-year PFS for the 94 patients who were age \geq 18 months at diagnosis and treated on CCG high-risk protocols was 23%. Among these patients, 30 (32%) had a low-risk score with a 5-year PFS rate of 47% (95% CI, 28% to 63%), and 64 (68%) had a high-risk score with a 5-year PFS of 12% (95% CI, 5% to 22%; $P = .002$), demonstrating that a subset of patients at extremely high risk of disease progression can be identified by the 14-gene signature among these otherwise clinically indistinguishable patients. Five-year OS for the 94 patients whose tumors had low- or high-risk scores also was significantly different (60% v 23%; $P = .003$; Data Supplement). Classification by resubstitution analysis showed higher accuracy in prediction and more divergent Kaplan-Meier curves (Data Supplement), reflecting the optimistically biased approach of this analysis and the need for cross validation.²⁴⁻²⁸

Independent validation of the 14-gene signature to predict PFS was obtained from analysis of metastatic NBL-NA tumors from two independent cohorts of patients (GPOH, n = 39; COG, n = 52) diagnosed at age \geq 18 months (Table 1; Data Supplement). Those patients whose tumors had signature-based high-risk scores had significantly worse 5-year PFS than those with low-risk scores (Figs 2C and 2D). Among the 39 GPOH patients, 21 (54%) had low-risk scores with a 5-year PFS rate of 57% (95% CI, 34% to 75%), and 18 (46%) had high-risk scores with a 5-year PFS of 8% (95% CI, 1% to 29%; $P = .002$). Nineteen COG patients (36%) had low-risk scores with a 5-year PFS rate of 50% (95% CI, 26% to 70%), and 33 (64%) had high-risk scores with a 5-year PFS of 20% (95% CI, 8% to 35%; $P = .009$). Five-year OS for patients in these two cohorts whose tumors had low- or high-risk scores also was significantly different (GPOH: 65% v 31%; $P = .012$; COG: 51% v 31%; $P = .039$; Data Supplement). These data show the validity of the 14-gene signature and the prognostic information obtained from inclusion of inflammation-related genes to identify subsets of patients with different outcomes in a clinically indistinguishable population.

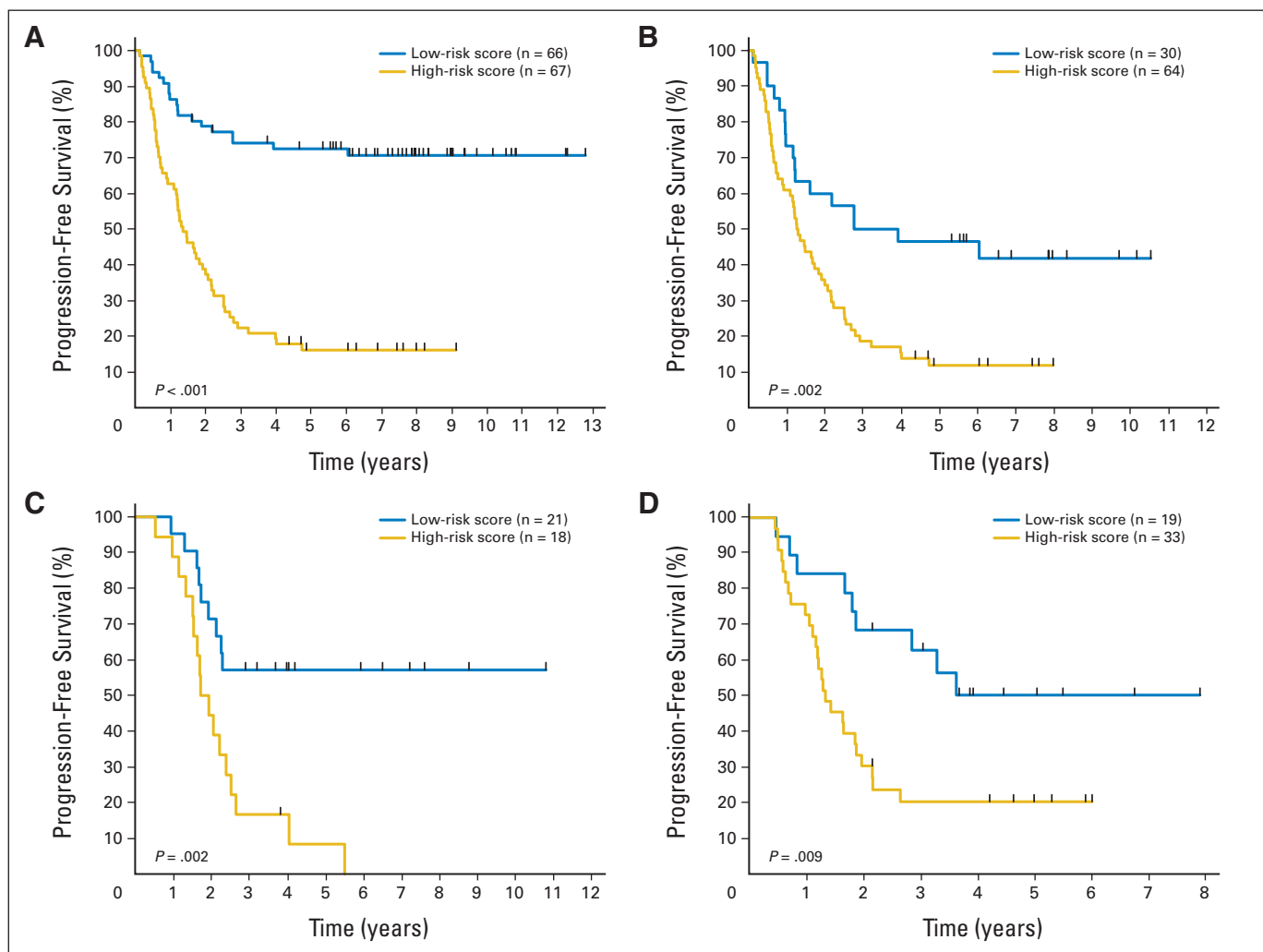


Fig 2. Progression-free survival (PFS) for patients in the training and validation cohorts with metastatic *MYCN*-nonamplified neuroblastoma (NBL-NA) 14-gene signature low- and high-risk scores. The cutoff value used to categorize patients into signature-based high- and low-risk score groups depended on the median score obtained in the Children's Cancer Group (CCG) cohort. The high-risk score group had prediction scores higher than the median score, whereas the low-risk score group had prediction scores lower than the median. The graphs show Kaplan-Meier estimates of PFS for patients with NBL-NA according to 14-gene signature risk classification. PFS estimates using the leave-one-out cross-validation signature classification for (A) the entire CCG cohort ($n = 133$) and (B) CCG patients diagnosed at age ≥ 18 months (clinically defined high-risk group; $n = 94$). The classification model developed using the CCG samples was then used to identify signature-based groups for patients age ≥ 18 months treated on (C) German Society for Pediatric Oncology-Hematology high-risk protocols ($n = 39$) and (D) Children's Oncology Group high-risk protocols ($n = 52$). All P values are based on log-rank test.

Prognostic Contribution of Genes Related to Tissue-Associated Macrophages

The five inflammation-related genes in our 14-gene model included *CD14*, *CD33*, *FCGR3* (*CD16*), interleukin-6 receptor (*IL6R*), and interleukin-10 (*IL10*), which are mainly expressed by macrophages and myeloid cells and, along with *CD163*, signify intratumor macrophage polarization to the anti-inflammatory M2-like phenotype.^{28,29} Our previous research demonstrated that expression of these inflammation-related genes in neuroblastoma tumors correlates with microscopic presence of *IL6*-producing CD68⁺ cells, which are considered to be TAMs.³⁰ Comparison of levels of expression of inflammation-related genes in neuroblastoma tumors with five neuroblastoma cell lines demonstrated that these markers are expressed 150-fold (range, five to 309; t test $P < .001$) higher on average in tumors than in cell lines (Fig 3B), suggesting that these genes are primarily expressed by tumor-associated inflammatory cells and consistent with IHC findings.

We next investigated the contribution of gene categories and age at diagnosis to the predictive accuracy of the NBL-NA signature. Using a permutation strategy (Data Supplement), we discovered that on average, the inclusion of inflammation-related genes explained 25% of the accuracy of the 14-gene model in predicting PFS and added to the 63% provided by tumor cell-related genes. Age at diagnosis explained an additional 12% of the accuracy.

Inflammation-related genes were also found to be highly correlated to one another in the CCG cohort, a pattern that was also observed in the GPOH and COG cohorts (Fig 3A; Data Supplement). The strongest gene-gene correlations were observed between *IL6R* and *CD14* (Spearman $r = 0.77$; $P < .001$; Fig 3C) and between *IL6R* and *CD33* (Spearman $r = 0.75$; $P < .001$). *IL6R* is primarily expressed on cells of the monocytic lineage, but it has also been reported to be expressed on some neuroblastoma cell lines.³¹

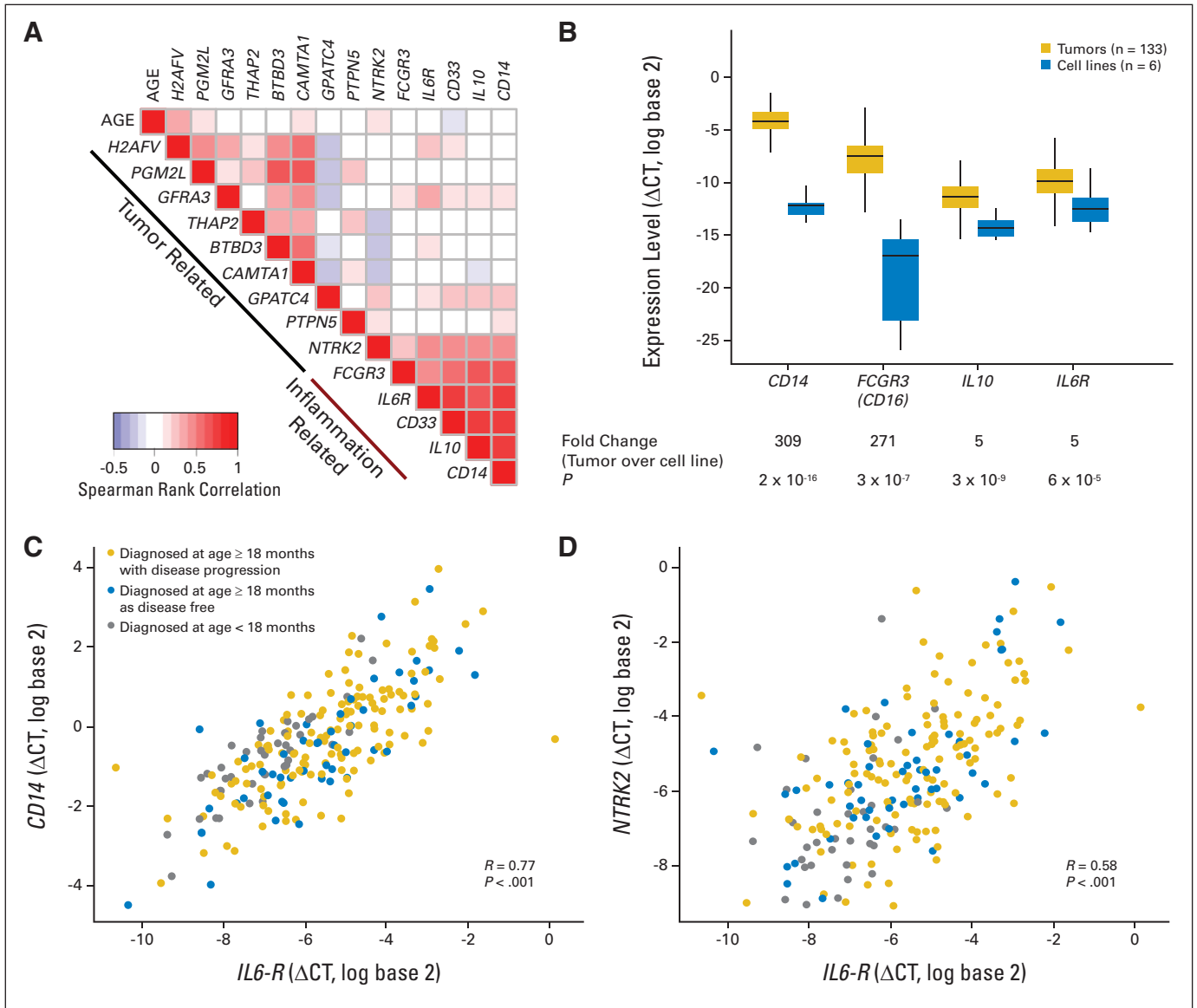


Fig 3. Inflammation- and tumor-related gene-gene correlations. (A) Heatmap of the Spearman rank correlation matrix of the 14 genes in the metastatic *MYCN*-nonamplified neuroblastoma (NBL-NA) signature. Pairwise rank correlation analyses were performed for all 14 genes and age at diagnosis. The patterns of correlation using samples from Children’s Cancer Group (CCG) patients diagnosed at age ≥ 18 months were similar to the pairwise rank correlations obtained using samples from the German Society for Pediatric Oncology-Hematology and Children’s Oncology Group validation cohorts (Data Supplement). Red represents positive rank correlation level above zero (white color) for a given gene pair, and blue represents negative rank correlation level. The inflammation-related genes (*FCGR3/CD16*, *CD33*, *CD14*, *IL6R*, *IL10*) show high levels of correlation across all cohorts. *NTRK2* has the strongest correlation of any tumor cell-related gene with inflammation-related genes. (B) Expression of inflammation-related genes is predominantly present in neuroblastoma tumors and not on cell lines. Normalized expression (Δ CT) values of four of the five inflammation-related genes (*CD14*, *FCGR3/CD16*, *IL10*, *IL6R*) in the CCG tumors ($n = 133$) were compared with six neuroblastoma *MYCN* nonamplified cell lines (CHLA-15, CHLA-20, CHLA-255, CHLA-42, CHLA-90, LAN-6). Data on the cell lines were generated on a TaqMan low-density array (Life Technologies, Carlsbad, CA) card that did not include *CD33* probes. On average, there was 309-, 271-, seven-, and five-fold higher expression of *CD14*, *FCGR3/CD16*, *IL10*, and *IL6R* in tumors than in cell lines, respectively, suggesting that these genes are primarily expressed by tumor-associated inflammatory cells. (C) Scatter diagram of expression of *CD14*, a macrophage marker, and *IL6R* reveals a high correlation in patients with metastatic NBL-NA. (D) Similarly, *NTRK2*, a tumor cell-related gene, shows moderate correlation with expression of *IL6R*, an inflammation-related gene. Gray, patients diagnosed at age < 18 months with metastatic NBL-NA; blue, disease-free patients diagnosed at age ≥ 18 months; gold, disease progression in patients diagnosed at age ≥ 18 months.

The nine genes categorized as tumor cell-related included neurotrophic kinase receptor 2 (*NTRK2*) and calmodulin-binding transcription activator 1 (*CAMTA1*), genes known to be associated with neuroblastoma growth and suppression, respectively.²⁴⁻²⁷ Interestingly, *IL6R* was also found to be moderately correlated with the expression of *NTRK2* (Spearman $r = 0.58$; $P < .001$; Fig 3D). Together, these data suggest that inflammation-related genes, especially genes

related to polarization of TAMs, contribute to prognosis and are associated with a poor clinical outcome.

DISCUSSION

The diverse outcomes of children with NBL-NA have been largely unexplained. Our study suggests for the first time that infiltrating

inflammatory cells, especially TAMs, may contribute to this diversity. We demonstrate that TAMs are more prevalent in tumors of children with metastatic rather than locoregional neuroblastoma. Furthermore, we show that expression of inflammation-related genes is higher in tumors of children diagnosed at age ≥ 18 months and that a subset of these genes representing TAMs is associated with an extremely poor outcome in this group. Including expression of both inflammatory and tumor cell genes in a 14-gene signature enables prediction of disease progression for the first time in the clinically indistinguishable group of patients diagnosed at age ≥ 18 months with metastatic NBL-NA. The novel finding that five inflammation-related genes contribute to 25% of the accuracy of the 14-gene model emphasizes the role of inflammation in neuroblastoma and uncovers previously unrecognized potential targets for therapy. This 14-gene expression scoring model, which was validated in two independent cohorts of patients, has clinical applicability and may be of use for managing high-risk patients.

In recent years, the concept of inflammatory cells in the tumor microenvironment as critical participants in tumor progression has gained acceptance.^{1,32} A tumor-infiltrating macrophage and T-cell signature ($CD68^{\text{high}}/CD4^{\text{high}}/CD8^{\text{low}}$) has been reported to predict PFS and OS in patients with breast cancer.⁴ In our study, *IL6R* expression was found to be highly correlated with expression of *CD14* (macrophage marker) and *CD33* (myeloid marker), and their expression, along with that of *IL10* and *FCGR3/CD16* (M2 polarization), contributed to the accuracy of our model in predicting disease progression. This novel finding provides a validated clinical context for the recently established role of TAMs and bone marrow mesenchymal stem cells in promoting neuroblastoma growth via activation of the *IL6/IL6R* pathway.^{30,31} Melanomas and myelomas, similar to neuroblastomas, have also been shown to co-opt their tumor microenvironment cells to produce *IL6*, leading to *STAT3* activation and promotion of tumor growth.^{30,31,33,34} Studies using immunocompetent mouse cancer models have demonstrated that antibody responses against transformed cells could lead to recruitment and polarization of macrophages, leading to production of cytokines such as *IL6*, *IL10*, and *IL4* that in turn stimulate tumor growth and angiogenesis.^{35,36} In the current study, using a highly specific and sensitive TLDA assay, expression of genes related to the humoral immune system was observed in children diagnosed at age ≥ 18 months but did not contribute to the final predictive model. Additional studies are needed to elucidate the role of antibody response in neuroblastoma and its relation to recruitment and polarization of TAMs.

Genes related to tumor cells contributed most to the accuracy of the 14-gene NBL-NA signature and included *NTRK2*, which binds brain-derived neurotrophic factor and plays an important role in the survival and differentiation of neuroblastoma cells.^{25,26,37,38} The association of high *NTRK2* expression with aggressive behavior in metastatic NBL-NA was previously reported by our group²¹ and is further supported in this study. Our present work also reveals a novel association between expression of *IL6R* and *NTRK2*. Although additional mechanistic studies are required to understand interactions between these two pathways, our data point to the role of a pro-tumor inflammatory microenvironment in enabling a highly aggressive neuroblastoma phenotype.

Several gene expression and genomic studies of neuroblastoma tumors obtained at diagnosis have previously reported associations

with patient outcome.^{20,39-43} However, these studies analyzed groups of patients who were heterogeneous with respect to *MYCN* gene amplification status, clinical stage, and age at diagnosis. Segmental genomic alterations identified in high-risk NBL-NA tumors have not been predictive of outcome in this high-risk group but have had clinical utility in children with intermediate-risk neuroblastoma.^{20,41,44-48}

Gene expression-based models built using neuroblastoma samples from clinically heterogeneous groups of patients lack predictive accuracy in those diagnosed at age ≥ 18 months with metastatic NBL-NA.^{42,43} Similarly, our previously reported 55-gene NBL-NA-specific microarray signature²¹ was not predictive of outcome for patients with *MYCN*-amplified tumors, which represent a distinct molecular subgroup of neuroblastomas (unpublished data).⁴⁹ Overall, these findings suggest that prognostic studies in neuroblastomas should focus on well-defined molecular and clinical subgroups (eg, using *MYCN* status). Our current finding also highlights the importance of assessing the neuroblastoma tumor microenvironment in prognostic studies.

Our current study defines a clinically applicable 14-gene expression signature that identifies two subsets of patients with different PFS. Children with high-risk tumor-progression scores uniformly had a poor outcome, with 8% to 20% PFS at 5 years after diagnosis, whereas those with low-risk scores had 47% to 57% PFS. It is possible that the addition of treatment response evaluations such as imaging with ¹²³I-metaiodobenzylguanidine and quantification of bone marrow disease with polymerase chain reaction assays will further improve risk classification, especially for patients with a low-risk tumor-progression score.^{50,51}

In summary, our study reports the first evidence of a role for intratumor inflammation in metastatic neuroblastomas and provides a validated prognostic signature for children with metastatic NBL-NA. The increase in expression of inflammation-related genes in children age ≥ 18 months with poor outcome allows the identification of a subgroup of patients at extremely high risk who may benefit from treatments targeting the tumor microenvironment along with tumor cells. The recent success of therapies directed at tumor-associated immune system cells in adult cancers⁵²⁻⁵⁴ suggests opportunities for their application in children with neuroblastoma.

AUTHORS' DISCLOSURES OF POTENTIAL CONFLICTS OF INTEREST

The author(s) indicated no potential conflicts of interest.

AUTHOR CONTRIBUTIONS

Conception and design: Shahab Asgharzadeh, Robert C. Seeger
Collection and assembly of data: Shahab Asgharzadeh, Jill A. Salo, André Oberthuer, Matthias Fischer, Frank Berthold, Michael Hadjidaniel, Cathy Wei-Yao Liu, Leonid S. Metelista, Roger Pique-Regi, Peter Wakamatsu, Judith G. Villablanca, Susan G. Kreissman, Katherine K. Matthay, Hiroyuki Shimada, Wendy B. London, Richard Spoto, Robert C. Seeger
Data analysis and interpretation: Shahab Asgharzadeh, Jill A. Salo, Lingyun Ji, Michael Hadjidaniel, Roger Pique-Regi, Hiroyuki Shimada, Wendy B. London, Richard Spoto, Robert C. Seeger
Manuscript writing: All authors
Final approval of manuscript: All authors

REFERENCES

1. Hanahan D, Weinberg RA: Hallmarks of cancer: The next generation. *Cell* 144:646-674, 2011
2. Steidl C, Lee T, Shah SP, et al: Tumor-associated macrophages and survival in classic Hodgkin's lymphoma. *N Engl J Med* 362:875-885, 2010
3. Ueno T, Toi M, Saji H, et al: Significance of macrophage chemoattractant protein-1 in macrophage recruitment, angiogenesis, and survival in human breast cancer. *Clin Cancer Res* 6:3282-3289, 2000
4. DeNardo DG, Brennan DJ, Rexhepaj E, et al: Leukocyte complexity predicts breast cancer survival and functionally regulates response to chemotherapy. *Cancer Discov* 1:54-67, 2011
5. Bronkhorst IH, Ly LV, Jordanova ES, et al: Detection of M2-macrophages in uveal melanoma and relation with survival. *Invest Ophthalmol Vis Sci* 52:643-650, 2011
6. Kurahara H, Shinchi H, Mataka Y, et al: Significance of M2-polarized tumor-associated macrophage in pancreatic cancer. *J Surg Res* 167:e211-e219, 2011
7. Cohn SL, Pearson AD, London WB, et al: The International Neuroblastoma Risk Group (INRG) classification system: An INRG Task Force report. *J Clin Oncol* 27:289-297, 2009
8. Deyell RJ, Attiyeh EF: Advances in the understanding of constitutional and somatic genomic alterations in neuroblastoma. *Cancer Genet* 204:113-121, 2011
9. Schmidt ML, Lukens JN, Seeger RC, et al: Biologic factors determine prognosis in infants with stage IV neuroblastoma: A prospective Children's Cancer Group study. *J Clin Oncol* 18:1260-1268, 2000
10. Matthay KK, Reynolds CP, Seeger RC, et al: Long-term results for children with high-risk neuroblastoma treated on a randomized trial of myeloablative therapy followed by 13-cis-retinoic acid: A Children's Oncology Group study. *J Clin Oncol* 27:1007-1013, 2009
11. Simon T, Hero B, Faldum A, et al: Long term outcome of high-risk neuroblastoma patients after immunotherapy with antibody ch14.18 or oral metronomic chemotherapy. *BMC Cancer* 11:21, 2011
12. Berthold F, Boos J, Burdach S, et al: Myeloablative megatherapy with autologous stem-cell rescue versus oral maintenance chemotherapy as consolidation treatment in patients with high-risk neuroblastoma: A randomised controlled trial. *Lancet Oncol* 6:649-658, 2005
13. Cheung NK, Kushner BH, Kramer K: Monoclonal antibody-based therapy of neuroblastoma. *Hematol Oncol Clin North Am* 15:853-866, 2001
14. Matthay KK, Villablanca JG, Seeger RC, et al: Treatment of high-risk neuroblastoma with intensive chemotherapy, radiotherapy, autologous bone marrow transplantation, and 13-cis-retinoic acid: Children's Cancer Group. *N Engl J Med* 341:1165-1173, 1999
15. George RE, Li S, Medeiros-Nancarrow C, et al: High-risk neuroblastoma treated with tandem autologous peripheral-blood stem cell-supported transplantation: Long-term survival update. *J Clin Oncol* 24:2891-2896, 2006
16. Yu AL, Gilman AL, Ozkaynak MF, et al: Anti-GD2 antibody with GM-CSF, interleukin-2, and isotretinoin for neuroblastoma. *N Engl J Med* 363:1324-1334, 2010
17. Schmidt ML, Lal A, Seeger RC, et al: Favorable prognosis for patients 12 to 18 months of age with stage 4 nonamplified MYCN neuroblastoma: A Children's Cancer Group Study. *J Clin Oncol* 23:6474-6480, 2005
18. Baker DL, Schmidt ML, Cohn SL, et al: Outcome after reduced chemotherapy for intermediate-risk neuroblastoma. *N Engl J Med* 363:1313-1323, 2010
19. George RE, London WB, Cohn SL, et al: Hyperdiploidy plus nonamplified MYCN confers a favorable prognosis in children 12 to 18 months old with disseminated neuroblastoma: A Pediatric Oncology Group study. *J Clin Oncol* 23:6466-6473, 2005
20. Janoueix-Lerosey I, Schleiernacher G, Michels E, et al: Overall genomic pattern is a predictor of outcome in neuroblastoma. *J Clin Oncol* 27:1026-1033, 2009
21. Asgharzadeh S, Pique-Regi R, Sposto R, et al: Prognostic significance of gene expression profiles of metastatic neuroblastomas lacking MYCN gene amplification. *J Natl Cancer Inst* 98:1193-1203, 2006
22. Kalbfleisch J, Prentice R: *The Statistical Analysis of Failure Time Data*. New York, NY, John Wiley and Sons, 1980
23. Mood AM, Garybill FA, Boes DC: *Introduction to the Theory of Statistics*. New York, NY, McGraw-Hill, 1974
24. Katoh M, Katoh M: Identification and characterization of FLJ10737 and CAMTA1 genes on the commonly deleted region of neuroblastoma at human chromosome 1p36.31-p36.23. *Int J Oncol* 23:1219-1224, 2003
25. Nakagawara A, Azar CG, Scavarda NJ, et al: Expression and function of TRK-B and BDNF in human neuroblastomas. *Mol Cell Biol* 14:759-767, 1994
26. Nakagawara A, Arima-Nakagawara M, Scavarda NJ, et al: Association between high levels of expression of the TRK gene and favorable outcome in human neuroblastoma. *N Engl J Med* 328:847-854, 1993
27. Henrich KO, Fischer M, Mertens D, et al: Reduced expression of CAMTA1 correlates with adverse outcome in neuroblastoma patients. *Clin Cancer Res* 12:131-138, 2006
28. Biswas SK, Mantovani A: Macrophage plasticity and interaction with lymphocyte subsets: Cancer as a paradigm. *Nat Immunol* 11:889-896, 2010
29. Leidi M, Gotti E, Bologna L, et al: M2 macrophages phagocytose rituximab-opsonized leukemic targets more efficiently than m1 cells in vitro. *J Immunol* 182:4415-4422, 2009
30. Song L, Asgharzadeh S, Salo J, et al: V α 24-invariant NKT cells mediate antitumor activity via killing of tumor-associated macrophages. *J Clin Invest* 119:1524-1536, 2009
31. Ara T, Song L, Shimada H, et al: Interleukin-6 in the bone marrow microenvironment promotes the growth and survival of neuroblastoma cells. *Cancer Res* 69:329-337, 2009
32. Tan TT, Coussens LM: Humoral immunity, inflammation and cancer. *Curr Opin Immunol* 19:209-216, 2007
33. Bromberg JF, Wrzeszczynska MH, Devgan G, et al: Stat3 as an oncogene. *Cell* 98:295-303, 1999
34. Klein B, Zhang X, Jourdan M, et al: Paracrine rather than autocrine regulation of myeloma-cell growth and differentiation by interleukin-6. *Blood* 73:517-526, 1989
35. de Visser KE, Korets LV, Coussens LM: De novo carcinogenesis promoted by chronic inflammation is B lymphocyte dependent. *Cancer Cell* 7:411-423, 2005
36. Andreu P, Johansson M, Affara NI, et al: FcR-gamma activation regulates inflammation-associated squamous carcinogenesis. *Cancer Cell* 17:121-134, 2010
37. Suzuki T, Bogenmann E, Shimada H, et al: Lack of high-affinity nerve growth factor receptors in aggressive neuroblastomas. *J Natl Cancer Inst* 85:377-384, 1993
38. Aoyama M, Asai K, Shishikura T, et al: Human neuroblastomas with unfavorable biologies express high levels of brain-derived neurotrophic factor mRNA and a variety of its variants. *Cancer Lett* 164:51-60, 2001
39. Ohira M, Nakagawara A: Global genomic and RNA profiles for novel risk stratification of neuroblastoma. *Cancer Sci* 101:2295-2301, 2010
40. Fischer M, Spitz R, Oberthür A, et al: Risk estimation of neuroblastoma patients using molecular markers. *Klin Padiatr* 220:137-146, 2008
41. Attiyeh EF, London WB, Mossé YP, et al: Chromosome 1p and 11q deletions and outcome in neuroblastoma. *N Engl J Med* 353:2243-2253, 2005
42. Oberthür A, Hero B, Berthold F, et al: Prognostic impact of gene expression-based classification for neuroblastoma. *J Clin Oncol* 28:3506-3515, 2010
43. De Preter K, Vermeulen J, Brors B, et al: Accurate outcome prediction in neuroblastoma across independent data sets using a multigene signature. *Clin Cancer Res* 16:1532-1541, 2010
44. Guo C, White PS, Hogarty MD, et al: Deletion of 11q23 is a frequent event in the evolution of MYCN single-copy high-risk neuroblastomas. *Med Pediatr Oncol* 35:544-546, 2000
45. Plantaz D, Vandesompele J, Van Roy N, et al: Comparative genomic hybridization (CGH) analysis of stage 4 neuroblastoma reveals high frequency of 11q deletion in tumors lacking MYCN amplification. *Int J Cancer* 91:680-686, 2001
46. Bagatell R, Rumcheva P, London WB, et al: Outcomes of children with intermediate-risk neuroblastoma after treatment stratified by MYCN status and tumor cell ploidy. *J Clin Oncol* 23:8819-8827, 2005
47. Bown N, Cotterill S, Lastowska M, et al: Gain of chromosome arm 17q and adverse outcome in patients with neuroblastoma. *N Engl J Med* 340:1954-1961, 1999
48. Carén H, Kryh H, Nethander M, et al: High-risk neuroblastoma tumors with 11q-deletion display a poor prognostic, chromosome instability phenotype with later onset. *Proc Natl Acad Sci* 107:4323-4328, 2010
49. Guo X, Chen QR, Song YK, et al: Exon array analysis reveals neuroblastoma tumors have distinct alternative splicing patterns according to stage and MYCN amplification status. *BMC Med Genomics* 4:35, 2011
50. Beiske K, Burchill SA, Cheung IY, et al: Consensus criteria for sensitive detection of minimal neuroblastoma cells in bone marrow, blood and stem cell preparations by immunocytology and QRT-PCR: Recommendations by the International Neuroblastoma Risk Group Task Force. *Br J Cancer* 100:1627-1637, 2009
51. Naranjo A, Parisi MT, Shulkin BL, et al: Comparison of ¹²³I-metaiodobenzylguanidine (MIBG) and ¹³¹I-MIBG semi-quantitative scores in predicting survival in patients with stage 4 neuroblastoma: A report from the Children's Oncology Group. *Pediatr Blood Cancer* 56:1041-1045, 2011
52. Hodi FS, O'Day SJ, McDermott DF, et al: Improved survival with ipilimumab in patients with metastatic melanoma. *N Engl J Med* 363:711-723, 2010
53. Beatty GL, Chioarean EG, Fishman MP, et al: CD40 agonists alter tumor stroma and show efficacy against pancreatic carcinoma in mice and humans. *Science* 331:1612-1616, 2011
54. Brahmer JR, Drake CG, Wollner I, et al: Phase I study of single-agent anti-programmed death-1 (MDX-1106) in refractory solid tumors: Safety, clinical activity, pharmacodynamics, and immunologic correlates. *J Clin Oncol* 28:3167-3175, 2010